Molecular Biology of the Cell
Vol. 15, 268–280, January 2004

Targeting of a Tropomyosin Isoform to Short Microfilaments Associated with the Golgi Complex

Justin M. Percival,[*†‡] Julie A. I. Hughes,[*†] Darren L. Brown,[§] Galina Schevzov,[*†] Kirsten Heimann,[§¶] Bernadette Vrhovski,[*] Nicole Bryce,[*†] Jennifer L. Stow,[§‖] and Peter W. Gunning[*†#]

[*]Oncology Research Unit, The Children's Hospital at Westmead, Westmead, NSW 2145, Australia;
[†]Discipline of Paediatrics and Child Health, University of Sydney, Sydney, NSW 2006, Australia;
[§]Institute for Molecular Bioscience, University of Queensland, Brisbane, QLD 4072, Australia; and
[‖]School of Molecular and Microbial Sciences, University of Queensland, Brisbane, QLD 4072, Australia

Submitted March 26, 2003; Revised August 8, 2003; Accepted August 26, 2003
Monitoring Editor: David Drubin

A growing body of evidence suggests that the Golgi complex contains an actin- based filament system. We have previously reported that one or more isoforms from the tropomyosin gene Tm5NM (also known as γ-Tm), but not from either the α- or β-Tm genes, are associated with Golgi-derived vesicles (Heimann *et al.*, (1999). J. Biol. Chem. *274*, 10743–10750). We now show that Tm5NM-2 is sorted specifically to the Golgi complex, whereas Tm5NM-1, which differs by a single alternatively spliced internal exon, is incorporated into stress fibers. Tm5NM-2 is localized to the Golgi complex consistently throughout the G1 phase of the cell cycle and it associates with Golgi membranes in a brefeldin A–sensitive and cytochalasin D–resistant manner. An actin antibody, which preferentially reacts with the ends of microfilaments, newly reveals a population of short actin filaments associated with the Golgi complex and particularly with Golgi-derived vesicles. Tm5NM-2 is also found on these short microfilaments. We conclude that an alternative splice choice can restrict the sorting of a tropomyosin isoform to short actin filaments associated with Golgi-derived vesicles. Our evidence points to a role for these Golgi-associated microfilaments in vesicle budding at the level of the Golgi complex.

INTRODUCTION

The actin microfilament system performs a broad range of cellular functions from regulating cell structure to cell motility and cytokinesis. The ability of microfilaments to independently perform such a broad array of functions may be facilitated by the sorting of isoforms of the primary components of microfilaments to different intracellular compartments. Actin, which provides the core microfilament polymer, is encoded by two isoforms in mammalian nonmuscle cells (Herman, 1993). Many microfilaments contain tropomyosin (Tm), a coiled coil protein that binds along the side of actin filaments (Phillips *et al.*, 1979). There are at least 40 different isoforms of tropomyosin (Lees-Miller and Helfman, 1991; Dufour *et al.*, 1998). Thus the potential for creation of microfilaments with unique actin and tropomyosin isoform composition is very extensive.

Studies in a variety of systems have provided consistent evidence for sorting of actin and tropomyosin isoforms to different intracellular locations (reviewed in Lin *et al.*, 1997; Gunning *et al.*, 1998a, 1998b). Isoform sorting, coupled to different functional properties of actin and tropomyosins, provide an attractive approach for spatially specializing microfilament function (Gunning *et al.*, 1998a). Nonmuscle tropomyosin isoforms protect actin filaments from severing (Burgess *et al.*, 1987; Ishikawa *et al.*, 1989). Tropomyosins regulate actin filament dynamics by affecting the activity of ADF/cofilin and the Arp 2/3 complex (Bamburg, 1999; Blanchoin *et al.*, 2001; Ono and Ono, 2002) in an isoform specific manner (Bryce *et al.*, 2003). They can also regulate actin filament organization by competing for binding with actin bundling proteins (Ishikawa *et al.*, 1994), controlling myosin motor activity in an isoform-specific manner (Fanning *et al.*, 1994; Strand *et al.*, 2001; Tang and Ostap, 2001) and can specify isoform sorting of myosins (Bryce *et al.*, 2003). Tm5NM-1 slows actin depolymerization and may play a role as a molecular ruler for actin filament length in conjunction with tropomodulin (Broschat, 1990; Fowler, 1996; Sung *et al.*, 2000). Taken together, there is now strong evidence that isoform sorting targets isoforms with different properties to different compartments. This may be an ancient mechanism to spatially specialize microfilament function because yeast, with only two tropomyosin isoforms partially sorts these isoforms and gene deletion studies indicate they are not functionally redundant (Drees *et al.*, 1995).

Recent reports implicate actin and many of its binding partners in Golgi complex–mediated trafficking. Nonmuscle actin and actin-binding proteins associate with Golgi membranes and vesicles in mammalian cells. These include my-

Article published online ahead of print. Mol. Biol. Cell 10.1091/mbc.E03–03–0176. Article and publication date are available at www.molbiolcell.org/cgi/doi/10.1091/mbc.E03–03–0176.

[#] Corresponding author. E-mail address: peterg3@chw.edu.au.
Present addresses: [‡] Department of Physiology and Biophysics, University of Washington, Seattle, WA 98195-7290; [¶] School of Tropical Biology, James Cook University, Townsville, QLD 4811, Australia.

Abbreviations used: BFA, brefeldin A; Tm, tropomyosin; ARF, ADP-ribosylation factor.

osin II, β-spectrin, ankyrin, β- and γ-actin, Tm5NM-1 and/or -2, drebrin, gelsolin, and profilin (Beck *et al.*, 1994, 1997; Devarajan *et al.*, 1996; Ikonen *et al.*, 1997; Heimann *et al.*, 1999; Lorra and Huttner, 1999; Dong *et al.*, 2000; Fucini *et al.*, 2000; Valderrama *et al.*, 2000). Actin, myosin II, myosin V, Tpm1p, gelsolin, and profilin have been implicated in post-Golgi trafficking in yeast and mammalian cells (Musch *et al.*, 1997; Hirschberg *et al.*, 1998; Pruyne *et al.*, 1998; Stow *et al.*, 1998; Heimann *et al.*, 1999; Lorra and Huttner, 1999). Nonmuscle actin is involved in the positioning and morphology of the Golgi complex and Golgi-to-ER retrograde trafficking (Valderrama *et al.*, 1998, 2001; Luna *et al.*, 2002). Specific pools of Golgi-associated actin, recruited by ARF1, assemble on Golgi membranes for roles in vesicle budding (Fucini *et al.*, 2000, 2002).

We previously reported that one or more isoforms from the Tm5NM gene (but not from the α- or β-Tm genes) are associated with Golgi-derived vesicles (Heimann *et al.*, 1999). In the present study we investigate the nature of the tropomyosins associated with the Golgi complex and we show that the restricted targeting of the Tm5NM-2 isoform to the Golgi complex is dependent on an internal alternatively spliced exon. In characterizing antibody-defined microfilaments we show the presence of a population of short actin filaments, also defined by Tm5NM-2, specifically concentrated around the Golgi complex. These data are consistent with a specific role for these microfilaments at one or more stages of vesicle budding from the Golgi complex.

MATERIALS AND METHODS

Antibodies

The primary rabbit antibody WS5/9d (Hannan *et al.*, 1995; Weinberger *et al.*, 1996) was used at 1:250 dilution. γ/9d is a polyclonal sheep antibody, made using a synthesized peptide encoding the entire Tm5NM gene 9d coding region from the mouse (DKLKCTKEEHLCTQRMLDQTLLDLNEM) conjugated to diphtheria toxin (Mimotopes, Clayton, Victoria, Australia). The peptide was injected into a sheep in four equal doses of 1.3 mg by the Institute for Medical and Veterinary Sciences, Veterinary Sciences Division (Adelaide, Australia) following their standard protocol. A total of 5 ml serum was affinity-purified using a column with Sepharose beads coupled to the peptide (Mimotopes). The antibody was used at 1/200 for Western blot and 1/100 for immunostaining. The mAb CG3 was a kind gift of J. Lin (Iowa). Anti-FTCD Golgi marker (also known as anti-58K, clone 58K-9) was purchased from Sigma Biosciences (St. Louis, MO). Anti-gly245 antibody has also been described previously (Leavitt *et al.*, 1987) and was a kind gift of U. Abei (Basel, Switzerland). Anti-p230 and anti-GM130 monoclonal antibodies were obtained from Transduction Laboratories (Lexington, KY).

Bacterial Expression of Tm5NM-1

The pPROEX HT prokaryotic expression system (Life Technologies, Invitrogen, Sydney, Australia) was used for the production of recombinant Tm5NM-1 protein. The Tm5NM-1 cDNA was PCR amplified from the pGEX expression vector kindly supplied by D. Helfman (Cold Spring Harbor, NY) and cloned into the pPROEX HT vector using restriction enzymes engineered into the PCR primers. Expression constructs were verified by sequencing. Induction of recombinant pPROEX HT clones was done according to the protocols outlined by Life Technologies, Invitrogen. In brief, the DH5α strain of *Escherchia coli* carrying the TM constructs were cultured in the presence of 100 μg/ml ampicillin to a density of A_{590} of 0.5–1.0. To induce expression of the recombinant Tm protein, isopropyl-β-D-thiogalactopyranoside was added to a final concentration of 0.6 mM. A 1-ml aliquot of cells was removed before and after 2-h induction and the absorbance, A_{600}, measured. The cells were centrifuged and resuspended in 100 μl of 2× SDS sample buffer (125 mM Tris-HCl, pH 6.8, 4% [wt/vol] SDS, 20% [vol/vol] glycerol, 0.01% [wt/vol] bromophenol blue). Samples were boiled and analyzed by SDS-PAGE.

Gel Electrophoresis and Western Blots

NIH 3T3 fibroblasts were cultured in vitro, washed with PBS, and lysed in SDS solubilization buffer (10 mM Tris, pH 7.6, 2% SDS, 2 mM dithiothreitol), and the extracts were heated at 95°C for 3 min. The proteins were precipitated as described by Wessel and Flugge (1984) and resolubilized in SDS solubilization buffer, and the protein concentration was determined by using a BCA Protein Assay Kit (Pierce, Rockford, IL). Before electrophoresis, protein samples were solubilized and boiled for 5 min in 2× sample buffer (1× buffer contains 0.125 M Tris, pH 6.8, 0.5% SDS, 5% glycerol, 5% 2-mercaptoethanol, 0.005% bromophenol blue). SDS-PAGE was performed according to Laemmli (1970) on 12.5% acrylamide and 0.1% bis-acrylamide. Prestained molecular weight markers were used (BenchMark PreStained Protein Ladder, Invitrogen Life Technologies). Proteins were transferred to Immobilon-P PVDF (Millipore Corp., Bedford, MA) for 1 h at 0.3 Amp, according to Towbin *et al.*, (1979). A 5% low fat skim milk in TBS (100 mM Tris HCl, pH 7.5, 150 mM NaCl) solution was used to block nonspecific binding on the blot. Primary and secondary (anti-rabbit and anti-sheep Ig-conjugated horseradish peroxidase, Amersham Bioscience, Castle Hill, Australia) antibodies were incubated for 1 h each, and four 15-min washes with TTBS (TBS with 0.05% Tween-20) were carried out after each antibody incubation. Blots were developed with the Western Lighting Chemiluminescence Reagent (Perkin Elmer-Cetus Life Sciences, Boston, MA) and exposed to Fuji X-ray film (Eastman Kodak, Rochester, NY).

Cell Culture and Transfections

NIH 3T3 fibroblasts were maintained at 50% confluence in Dulbecco's modified Eagle's medium (Invitrogen) supplemented with 10% fetal bovine serum (FBS) and 2 mM glutamine (Invitrogen) humidified with 5% CO_2. Madin-Darby canine kidney (MDCK) epithelial cells were grown and passaged from confluent monolayers as previously described (Miranda *et al.*, 2001). Synchronization of NIH 3T3 fibroblasts was performed as described in Percival *et al.* (2000). For staining, fibroblasts were grown on poly-L-lysine (Sigma Biosciences)–coated coverslips and glass chamber slides (Nalge Nunc International, Roskilde, Denmark) or on RS-coated (PLL analogue) Lab-Tek II chamber slides.

Plasmids were transfected into NIH 3T3 fibroblasts with FuGENE 6 transfection reagent (Roche Diagnostics, Castle Hill, Australia). Cells were incubated with FuGENE 6/DNA complexes for 24 h to allow for optimal expression. Brefeldin A (Sigma Biosciences) was stored as a 5 mg/ml stock solution in methanol and was diluted to the working concentration of 5 μg/ml with complete media. Cells were treated with brefeldin A (BFA) for 15 min and then washed three times with PBS and were incubated for a further hour in complete media. Cells were then washed and processed for confocal microscopy. Cytochalasin D (Sigma) was stored as a 2 mM stock solution in dimethyl sulfoxide and used at 2 μM. Cells were incubated with cytochalasin D for 1 h and then fixed. Nocodazole (Sigma Biosciences) was prepared as a 3 mM stock solution in dimethyl sulfoxide and diluted to 30 μM with complete media. Cells were incubated with nocodazole for 1 h and then fixed and immunolabeled as described below.

Immunofluorescence

Transiently transfected and drug-treated cells were washed three times with PBS without Ca^{2+} and Mg^{2+}. Then cells were fixed for 20 min at 4°C in freshly prepared 4% paraformaldehyde. Cells were permeabilized with chilled methanol (−20°C) for 20 min at 4°C or with 0.1% Triton X-100 (Sigma Biosciences) in PBS for 5 min. After permeabilization cell were rinsed three times with PBS without Ca^{2+} and Mg^{2+} and then blocked with 2% FBS in PBS for 5–10 min before addition of antibodies. Donkey anti-mouse, anti-rabbit, and anti-sheep IgG; goat anti-rabbit IgG; and sheep anti-mouse IgG Alexa 488– or Cy3–conjugated secondary antibodies were used to visualize primary antibodies (Jackson ImmunoResearch Laboratories, West Grove, PA). DAPI (Molecular Probes, Eugene, OR) was used to stain nuclei. Immunostained fibroblasts were mounted in antibleaching medium (100 μg/ml DABCO in 50% glycerol in PBS), coverslipped then analyzed by confocal laser scanning microscopy. All images were obtained sequentially with a TCS SP2 confocal laser scanning upright microscope (Leica Microsystems, Heidelberg, Germany) or by epifluorescence using an Olympus Provis AX-70 microscope (Olympus, Sydney, Australia) with image capture by a CCD300ET-RCX camera (DageMTI, Michigan City, IN).

Electron Microscopy and Immunogold Labeling

MDCK cells were grown to confluence and were processed for cryo-electron-microscopy or perforated for resin electronmicroscopy as previously described (Wylie *et al.*, 1999). For cell perforation, semidry filters (Millipore, Bedford, MA) were applied to the surface of cell monolayers and then ripped off. Cells were then incubated for 15 min in buffer containing an ATP-regenerating system, aluminum fluoride and concentrated cytosol. In some experiments, 10 μM Jasplakinolide (Molecular Probes) was added to the incubation buffer. Following incubation, the filters were fixed for 1 h with 4% paraformaldehyde in phosphate buffer and immunolabeled by floating on sequential drops of 0.02 M glycine, 1% BSA/PBS, primary antibody in 1% BSA/PBS (90 min), 1% BSA/PBS, 10 or 15 nm protein A-gold in 1% BSA/PBS (60 min), PBS, followed by a 5-min fixation in 1% glutaraldehyde in PBS. The labeling procedure was then repeated using a different primary antibody and different sized secondary conjugate. The filters were then fixed in 2.5% glutaraldehyde in sodium cacodylate buffer, processed for resin electronmicroscopy, and then sectioned using a Reicherdt Ultracut T ultramicrotome (Leica Microsystems, Rowville, Victoria, Australia) before viewing on a JEOL

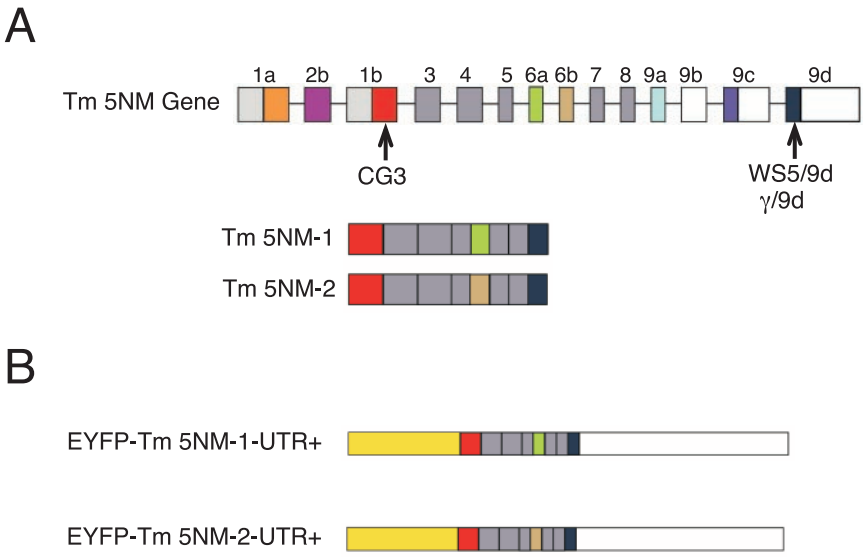

Figure 1. Tropomyosin gene organization and EYFP tropomyosin fusion constructs. (A) Organization of the *Tm5NM* gene (γ-Tm gene). Colored boxes represent exons and white boxes represent 3′ untranslated sequences. Light gray boxes represent 5′ untranslated sequences. The *Tm5NM* gene encodes Tm5NM-1 and -2, which are identical in amino acid sequence except at an internal alternatively spliced exon. Tm5NM-1 contains exon 6a, whereas Tm5NM-2 contains exon 6b. The recognition sites for the antibodies CG3, WS5/9d, and γ/9d are shown below the appropriate exon. (B) EYFP tropomyosin fusion constructs. Yellow rectangles representing EYFP are fused in frame to the amino termini of Tm5NM-1 and -2. White rectangles represent the 3′ untranslated (UTR) sequence from the 9d exon of the Tm5NM gene.

1010 Transmission electronmicroscope (JEOL Australasia, Brockswater, NSW, Australia) at 80 KeV.

Construction of EYFP Tropomyosin Fusion Plasmids

Total RNA was extracted from human fibroblasts using the RNeasy Mini Kit (Qiagen, Santa Clarita, CA) according to manufacturer's specifications. First-strand cDNA was synthesized from total RNA in a reaction primed by oligo $d(T)_{12–18}$ primers and catalyzed by Superscript II RNase H Reverse Transcriptase according to manufacturers specifications (Invitrogen). Tropomyosin cDNA templates were amplified using high fidelity Platinum *Pfx* DNA polymerase (Invitrogen) using tropomyosin sequence-specific primers. PCR amplification was performed on a Touchdown Thermal Cycling System (Hybaid Teddington, United Kingdom). Full-length Tm5NM-1 cDNA (Tm5NM-1-UTR+) including its entire 3′ untranslated region was amplified using an exon 1b sense primer with an extra *Bsp*EI site (5′-GTTCCGGAATGGCTGGGATCACCACC) and an antisense primer against the 3′ end of the UTR with an extra *Sal*I site (5′- ACGTCGACGAGGGTTGGAGGGACTGGTTC-3′). To amplify the full-length cDNA of hTm5NM-2, a two-step PCR strategy was used. To generate Tm5NM-2 full-length cDNA, a sense primer was designed that contained a *Bcl*I site at its 5′ end, which spanned the end of exon 5 and the first 23 bases of exon 6b (5′-AGTTGGTGATCATTGAAGGAG ACTTGGAACGCACAGAGGAACGAGCTGAGCTGGCAGAGTCAAATGTTCTGAGCTGGAGGAGGAG-3′). The same antisense primer was used as described for Tm5NM-1-UTR+. The *Bcl*I-*Sal*I fragment was amplified from the PCR reaction mixture obtained by the amplification of Tm5NM-1 described above. All PCR products were ligated into the pGEM-T cloning vector (Clontech, Palo Alto, CA). A schematic representation of the constructs used in this study is shown in Figure 1B. Tm5NM-1 cDNA was subcloned in frame into the *Bsp*EI and *Sal*I restriction sites of the pEYFP-C1 expression vector (Clontech) to create the pEYFP-Tm5NM-1 fusion protein (see Figure 1B). The *Bcl*I-*Sal*I fragment was cut out of pGEM-T containing Tm5NM-2 and subcloned between the *Bcl*I and *Sal*I sites of pEYFP-Tm5NM-1 to create pEYFP-Tm5NM-2 (Figure 1B). Both constructs were sequenced on an ABI 373 DNA automated sequencer using standard dye terminator technology (DNA Sequencing Facility, Westmead Millennium Institute).

RESULTS

An Internal Alternatively Spliced Exon Restricts Targeting of a Tm5NM Isoform to the Golgi Complex

We have previously shown that the antibody WS5/9d, which recognizes a subset of isoforms from the TM5NM gene, stains the Golgi compartment in quiescent NIH3T3 fibroblasts (Heimann *et al.*, 1999). The WS5/9d antibody was raised against the first six amino acids encoded by the 9d exon of the Tm5NM gene and therefore could react with one or both of the two Tm5NM isoforms, Tm5NM-1 and -2, which terminate with this coding exon (Figure 1). It has therefore been unclear which specific isoforms of Tm5NM associate with the Golgi complex. To further investigate this, we compared the cell staining patterns produced by WS5/9d and a new antibody (γ/9d) raised against the entire peptide encoded by the 9d exon of the Tm5NM gene. Both antibodies were found to have largely disparate staining patterns. The γ/9d antibody stains primarily stress fibers in 3T3 fibroblasts with less prominent staining of the perinuclear region (Figure 2A). WS5/9d produces only the characteristic perinuclear staining with no visible staining of stress fibers in these cells (Figure 2B). This indicates that either the WS5/9d epitope is masked in stress fibers or that WS5/9d and γ/9d differ in their recognition of the Tm5NM-1 and -2 isoforms.

Recently, we have shown that Tm5NM-1 transfected B35 cells localise this protein to stress fibres (Bryce *et al.*, 2003)

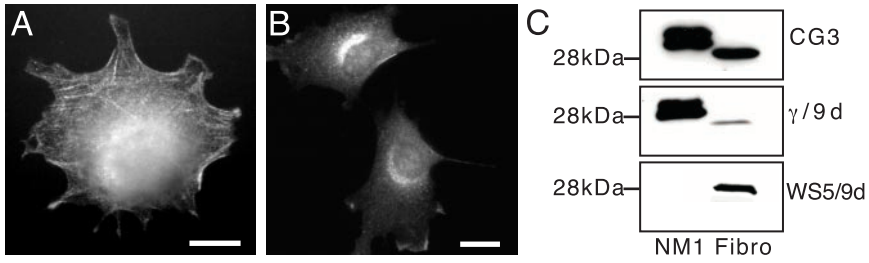

Figure 2. Tropomyosins Tm5NM-1 and -2 are differently targeted in NIH3T3 fibroblasts. NIH3T3 cells were stained with either WS5/9d or γ/9d antibodies. WS5/9d displays perinuclear staining (B), whereas γ/9d primarily stains stress fibers (A). Note that costaining with both antibodies produced very poor images and thus, only individually stained images are shown. (C) Western blots of fibroblast protein and bacterial extract expressing Tm5NM-1 were reacted with CG3, WS5/9d, and γ/9d. Note that unlike γ/9d, WS5/9d does not recognize Tm5NM-1. Scale bars, 15 μm.

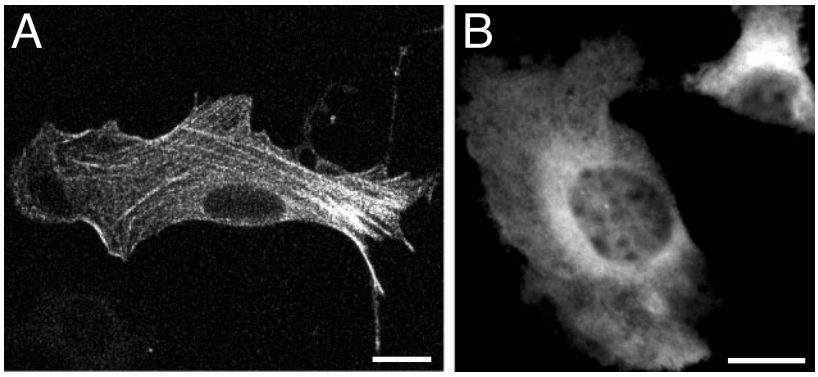

Figure 3. EYFP-Tm5NM-2 targets to a perinuclear compartment, whereas EYFP-Tm5NM-1 targets to stress fibers. Transient transfection of NIH3T3 fibroblasts with EYFP-Tm5NM-1-UTR+ for 24 h resulted in a predominantly stress fiber distribution (A), whereas cells transiently transfected with EYFP-Tm5NM-2-UTR+ plasmid for 24 h showed characteristic diffuse perinuclear targeting (B). EYFP-Tm5NM-2 was also often found associated with the leading edge. Scale bar, 15 μm.

and that WS5/9d does not detect the elevated protein level on Western blots (unpublished data). This suggests that WS5/9d does not detect Tm5NM-1. In order to test this, Tm5NM-1 was expressed in a bacterial expression system and electrophoresed adjacent to fibroblast protein. Parallel blots were reacted with CG3 (to show relative levels of bacterial Tm5NM-1 and total Tm5NM products in the fibroblasts), γ/9d and WS5/9d (Figure 2C). The CG3 antibody recognizes the characteristic Tm5NM products at about 30 kDa in the fibroblast lane and slightly larger bands in the Tm5NM-1 lane, corresponding to the his-tagged bacterial products. γ/9d recognizes the same bands detected by CG3 and the lower level of reaction in the fibroblasts is most likely due to expression of other Tm5NM products lacking the 9d carboxy terminus (Dufour *et al.,* 1998). In contrast, WS5/9d reacts strongly with the fibroblast sample at about 30 kDa but fails to show any cross-reactivity with Tm5NM-1. Interestingly, we have also recently observed similar isoform specificity comparing a mAb raised against the 9c exon of α-Tm to a polyclonal antibody raised against the whole 9c exon (Vrhovski *et al.,* 2003).

Taking these results together we conclude that the WS5/9d antibody primarily recognizes the Tm5NM-2 isoform and not Tm5NM-1, which is in stress fibers. Using WS5/9d we can detect Tm5NM-2 in cells, which is enriched around the perinuclear Golgi complex and is largely excluded from stress-fibers.

This specificity of Tm5NM-2 targeting and Golgi localization was further tested by transfecting tagged constructs (Figure 1B) of both isoforms into NIH3T3 fibroblasts. Tm5NM-1 tagged with EYFP produced images very similar to those seen with the γ/9d antibody in which the strongest staining is associated with stress-fibers (Figure 3A). In contrast, Tm5NM-2 tagged with EYFP failed to label stress fibers and revealed perinuclear staining similar, but not identical, to that observed with WS5/9d (Figure 3B). Because Tm5NM-1 and -2 differ by only one internal alternatively spliced exon (see Figure 1), we conclude that exon 6b promotes a preferred association with the Golgi complex and or inhibits incorporation into stress fibers.

Tm5NM-2 Associates with the Golgi Complex in an ARF1-dependent Manner

Previous studies have shown that during early G1, the different tropomyosin isoforms undergo extensive spatial reorganization (Percival *et al.,* 2000). We therefore costained synchronized cultures of NIH3T3 fibroblasts with WS5/9d and a Golgi marker to determine whether Tm5NM-2 undergoes similar reorganization or remains associated with the Golgi complex. WS5/9d stains a discrete, polarized, perinuclear compartment through the first 8 h of G1 and shows no detectable change during this time (Figure 4, E–H). The Golgi marker FTCD (Figure 4, A–D) shows coincident staining with WS5/9d at all times (Figure 4, I–L), suggesting that Tm5NM-2 is stably associated with the Golgi complex throughout G1 progression. The location of Tm5NM-2 at the Golgi complex was confirmed by costaining with another Golgi marker, GM130 (Nakamura *et al.,*1995). NIH3T3 fibroblasts showed striking colocalization of WS5/9d with GM130 (Figure 5).

Finally, the nature of the association of Tm5NM-2 with the Golgi complex was further tested using pharmacological agents which disrupt Golgi structure. Treatment of NIH3T3 fibroblasts for 15 min with BFA to disrupt ARF-dependent recruitment of vesicle-associated proteins resulted in a loss of perinuclear labeling and redistribution of WS5/9d staining to small cytoplasmic puncta (Figure 6B). Washout of BFA allowed reassembly of the Golgi complex and reestablishment of the perinuclear distribution of WS5/9d staining (Figure 6C). Parallel staining of cultures with the Golgi marker β-COP confirmed that 15-min treatment with BFA was sufficient to fully disperse β-COP, and 1 h after BFA washout β-COP displayed characteristic Golgi staining (Figure 6, D–F). This suggests that Tm5NM-2 is associated with membranes in the intact Golgi complex in an ARF1 GTPase-dependent manner, in a similar manner reported for other vesicle-associated proteins and, interestingly, pools of Golgi-associated actin (Fucini *et al.,* 2000).

The BFA sensitivity of EYFP-tagged Tm5NM-2 was also tested in NIH3T3 cells. Cells transiently transfected with EYFP-TmNM-2 displayed staining in a perinuclear location (Figure 6G) after transfection. Treatment of transfected cells with BFA for 15 min resulted in more dispersed staining throughout the cytoplasm (Figure 6H) and subsequent washout of the BFA resulted in restoration of the perinuclear distribution (Figure 6I). This suggests that the location of EYFP-Tm5NM-2 is regulated by ARF-1, in parallel with the regulation of endogenous Tm5NM-2.

Tm5NM-2 localization was also disrupted by treatment of cells with 30 μM nocodazole for 1 h (Figure 7, A and B). The large cytoplasmic puncta observed in treated cells (Figure 7B) is characteristic of the response of the Golgi complex to disruption of microtubules and further supports a bona fide association of Tm5NM-2 with the Golgi complex. In contrast, treatment with cytochalasin D was unable to alter WS5/9d staining at the Golgi complex (Figure 7, C and D), although this treatment largely eliminates stress fibers (Percival *et al.,* 2000). This is consistent with our previous observation that microfilaments containing Tm5NM isoforms are more resistant to cytochalasin

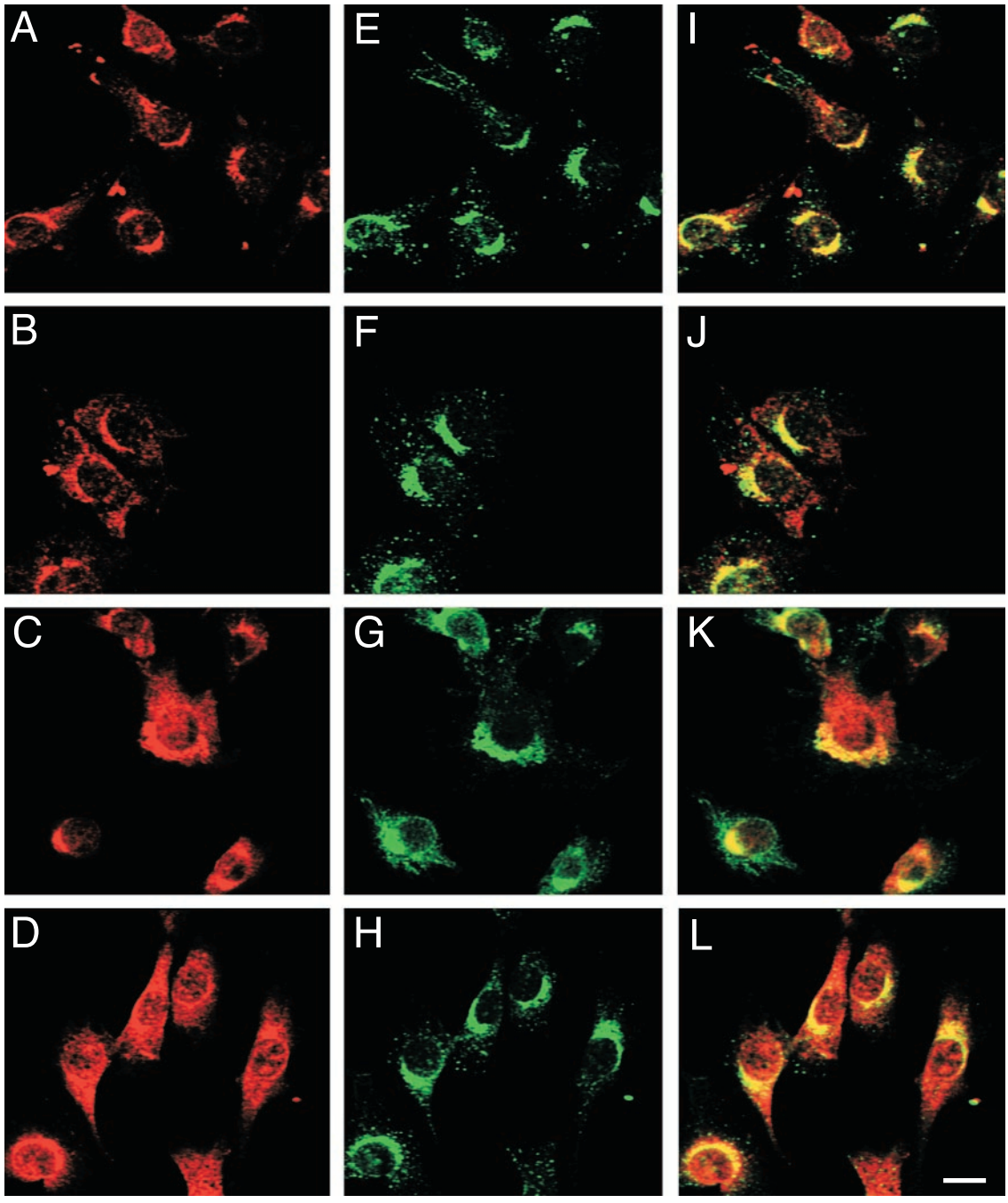

Figure 4. Tm5NM-2 colocalizes with the Golgi complex in synchonized NIH 3T3 fibroblasts. Fibroblasts in G0 and in G1 phases of the cell cycle were double-labeled with anti-FTCD (A–D) and WS5/9d (E–H) antibodies, their subcellular distributions were compared by confocal microscopy, and the merged images are shown (I–L). FTCD (A) and WS5/9d (E) colocalized to a perinuclear compartment in quiescent fibroblasts (I). FTCD and WS5/9d colocalized to the same perinuclear compartment at 3 (B, F, and J), 5 (C, G, and K), and 8 h (D, H, and L) into G1. FTCD protein is far more broadly distributed in the cytoplasm at 8 h (D) than WS5/9d (H), showing that Tm5NM-2 is not on all FTCD-positive structures. The overlapping distribution of Tm5NM-2 with FTCD in fibroblasts suggests that Tm5NM-2 is associated with the Golgi complex. Scale bars, 10 μm.

D than those containing tropomyosin isoforms from the α- and β- Tm genes (Percival *et al.*, 2000).

Short Actin Filaments and Tm5NM-2 Are Associated with Vesicles in the Golgi Complex

Because tropomyosins exist primarily attached to microfilaments, the presence of Tm5NM-2 around the Golgi complex is suggestive of some specialization of microfilaments in this region. Cell staining with different actin antibodies was performed. An antiactin serum (referred to here as anti-gly245) was previously generated against a 13 mer peptide corresponding to amino acids 239–251 of nonmuscle mammalian actin (Leavitt *et al.*, 1987). This region of actin lies at a major site of actin–actin subunit

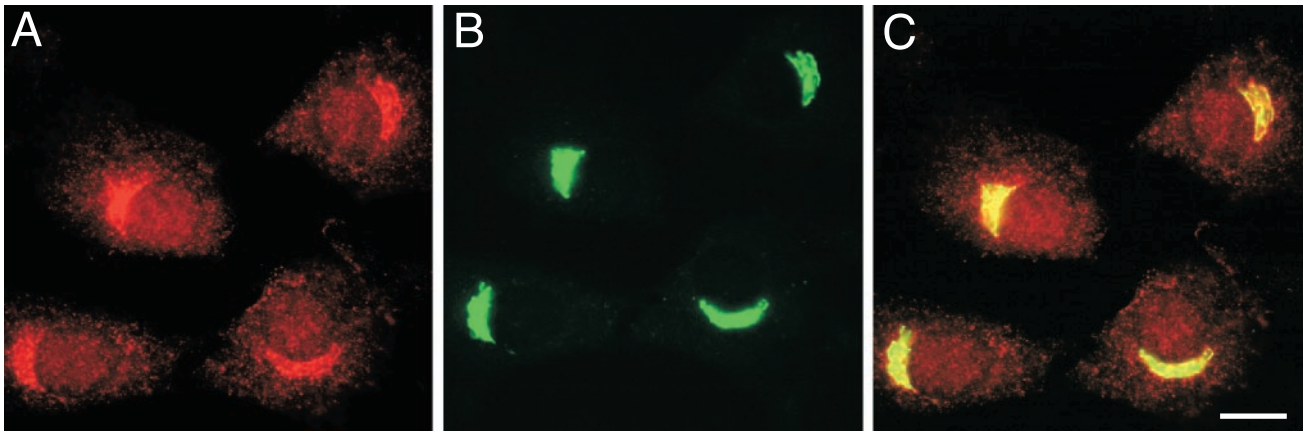

Figure 5. Tropomyosin Tm5NM-2 colocalizes with the Golgi marker GM130. NIH3T3 cells were costained with WS5/9d (A) and anti-GM130 (B) and the merged image is shown in C. The tight colocation confirms the presence of Tm5NM-2 in the Golgi complex. Scale bar, 15 μm.

contact (Steinmetz *et al.*, 1997), a site that would be expected to be obscured in polymers.

In our present studies, we found that the anti-gly245 antibody recognizes one major band corresponding to actin on a Western blot of NIH3T3 total cell lysate (Figure 8A). Cells were then costained with anti-gly245 and with a β-actin antibody that recognizes the amino terminus and should see all β-actin molecules in filaments. Comparison of the two distinct staining patterns reveals that, whereas the β-actin antibody primarily detects stress fibers (Figure 8B), anti-gly245 reacts largely with actin in a perinuclear compartment (Figure 8C). Careful examination does reveal that anti-gly245 also weakly detects some stress fibers (Figure 8C, top cell) and that anti–β-actin also produces weak staining of both a perinuclear compartment and cytoplasmic puncta (Figure 8B, lower cells). The colocation of perinuclear β-actin and anti-gly245 staining at these sites is shown in the merged image (Figure 8D). The data are therefore consistent with the prediction that anti-gly245 only poorly reacts with large actin polymers (such as those in stress fibers) and suggests that there is a high density of short actin filaments associated with a perinuclear compartment. Costaining of anti-gly245 (Figure 8F) and a Golgi marker (Figure 8E) indicates striking colocalization (Figure 8G), showing that the perinuclear, anti-gly245–labeled short actin filaments are primarily associated with the Golgi complex.

Labeling with anti-gly245 and with WS5/9d was then examined at an ultrastructural level on sections of perforated cells labeled by a preembedding immunogold technique. We performed this analysis using MDCK cells, whereas we have previously used this technique, which offers improved access to cytoplasmic, membrane-associated, and cytoskeletal proteins around the Golgi complex (Wylie *et al.*, 1999). First, we showed by immunofluorescence that the perinuclear staining of both anti-gly245 and WS5/9d is reproduced in intact MDCK cells and that this staining is also associated with the Golgi complex, labeled in this case for the TGN marker, p230 (Brown *et al.*, 2001; Figure 9). In perforated cells at an ultrastructural level, anti-gly245 labeling was seen as prominent gold particle decoration of microfilaments enmeshing the Golgi complex (Figure 10, A and C). Labeled actin filaments were particularly associated with clusters of vesicles or with the budding zones on the ends of cisternae, rather than with the cisternae of the Golgi stacks (Figure 10, B–E). Examples of individual Golgi-derived vesicles attached to short actin filaments are depicted in Figure 10. Vesicles attached to microfilaments were also double-labeled to detect other Golgi-associated motors. Figure 10F shows a vesicle surface-labeled for a myosin marker of TGN-derived vesicles, p200/myosinII (Ikonen *et al.*, 1997), and the attached microfilament is labeled with anti-gly245. In most sections the cell periphery contained only sparse examples of anti-gly245–labeled actin filaments and other organelles such as nuclei and mitochondria showed no specific labeling.

Immunogold labeling also confirmed that the anti-gly245 antibody preferentially detects the end of actin filaments. The location of anti-gly245 reactive actin appeared to be close to the ends of actin filaments rather than along the length of the filaments (see Figure 10). This was quantitated by measuring the frequency of immunogold labeling of ends vs. the middle of visible actin filaments. We found that 93% ($n = 372$) of filaments were labeled at the end(s), whereas only 7% were labeled along the length of the filaments. We conclude that the anti-gly 245 antibody does preferentially label the ends of actin filaments and this supports the suggestion from Figure 8 that the Golgi complex contains a high density of short actin filaments.

Short Actin Filaments Associated with Vesicles also Contain Tm5NM-2

Tm5NM-2 is associated with short actin filaments in the Golgi complex. Immunogold labeling of Tm5NM-2 using either WS5/9d or CG3 antibodies was associated with short Golgi microfilaments in the perinuclear area and with vesicles (Figure 11). In the micrographs in Figure 11 it is evident that Tm5NM-2 and anti-gly245 often colabel the same short microfilaments in the Golgi region and around vesicle clusters. The WS5/9d antibody was also used to label cryosections of intact, fixed cells, and although microfilaments are not visible in these preparations, there was labeling of coated vesicles (Figure 11D). Together these results confirm that Tm5NM-2 is associated with short microfilaments and with vesicles in and around the Golgi complex.

We previously showed that a Tm5NM gene product binds to a subset of Golgi vesicles during budding (Heimann *et al.*, 1999) and our current results suggest that Tm5NM-2 is on short actin filaments, which may also participate in vesicle budding. If so, then it might be expected that actin polymerization would enhance the budding process. We therefore

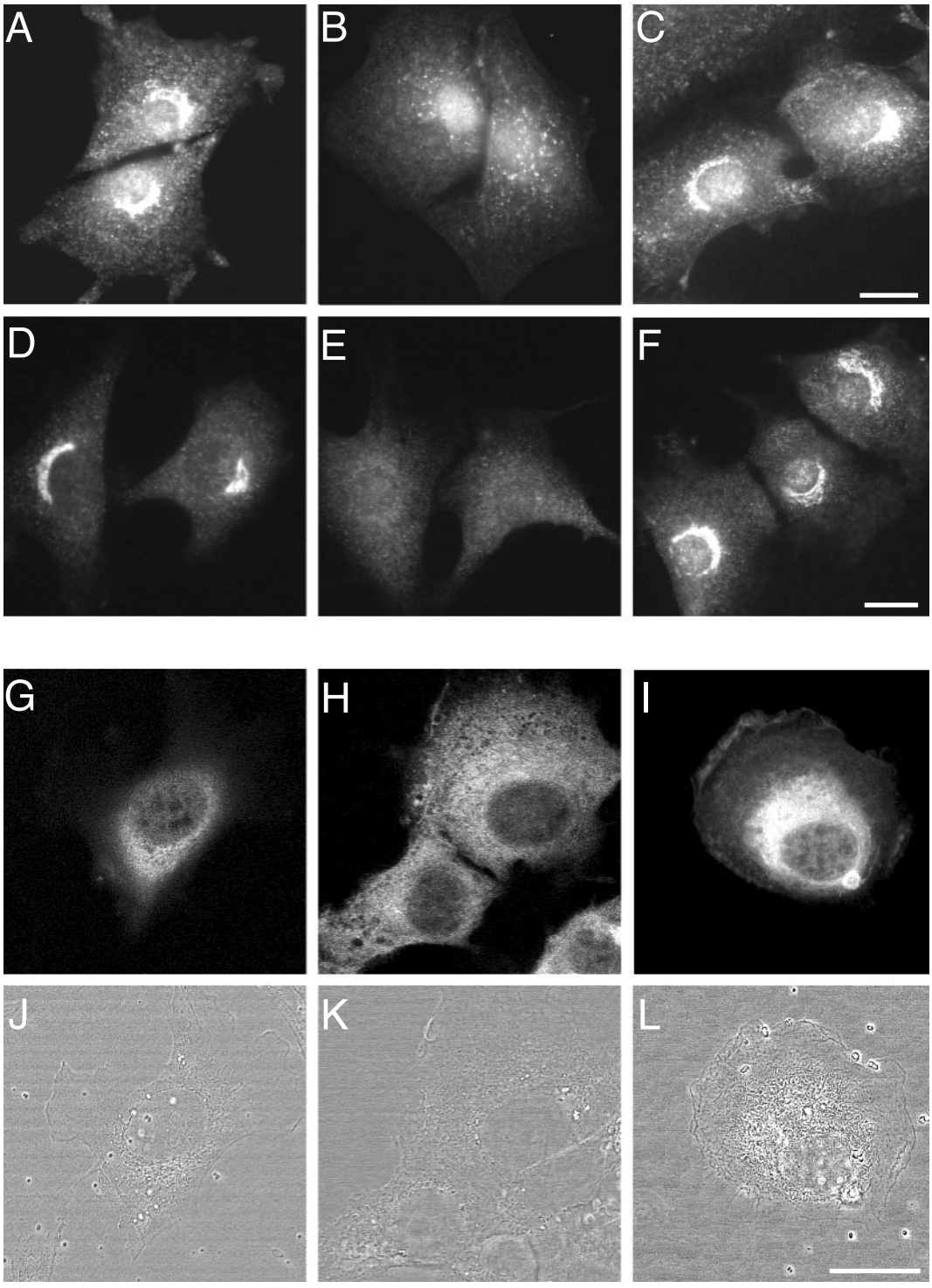

Figure 6. Tm5NM-2 labels the Golgi complex in a Brefeldin A–sensitive manner. Wild-type NIH3T3 cells (A–F) immunostained with WS5/9d or with β-COP antibodies and EYFP-Tm5NM-2 transfected NIH3T3 cells (G–L) were treated with vehicle alone (A, D, and G) or with BFA for 15 min (B, E, and H). Cells were also treated with BFA for 15 min, which was then washed out and followed by a 1-h recovery before fixation (C, F, and I). WS5/9d and β-COP antibody staining of parallel cultures shows perinuclear Golgi staining in both cases (A and D). BFA treatment caused loss of the characteristic perinuclear staining of WS5/9d (B) and β-COP (E). Washout of BFA allowed restoration of the characteristic perinuclear distribution of WS5/9d (C) and β-COP (F). In transfected cells the perinuclear distribution of EYFP-Tm5NM-2 (G) was similarly affected in the presence of BFA (H) and after BFA washout (I). Phase contrast images of the transfected cells in each case highlight the perinuclear concentration of EYFP-Tm5NM-2 (J and L) and its BFA-induced dispersal into the cell periphery (K). Note that lighter exposure of the image shown in H never resembled the patterns shown in G or I. Scale bars, 15 μm.

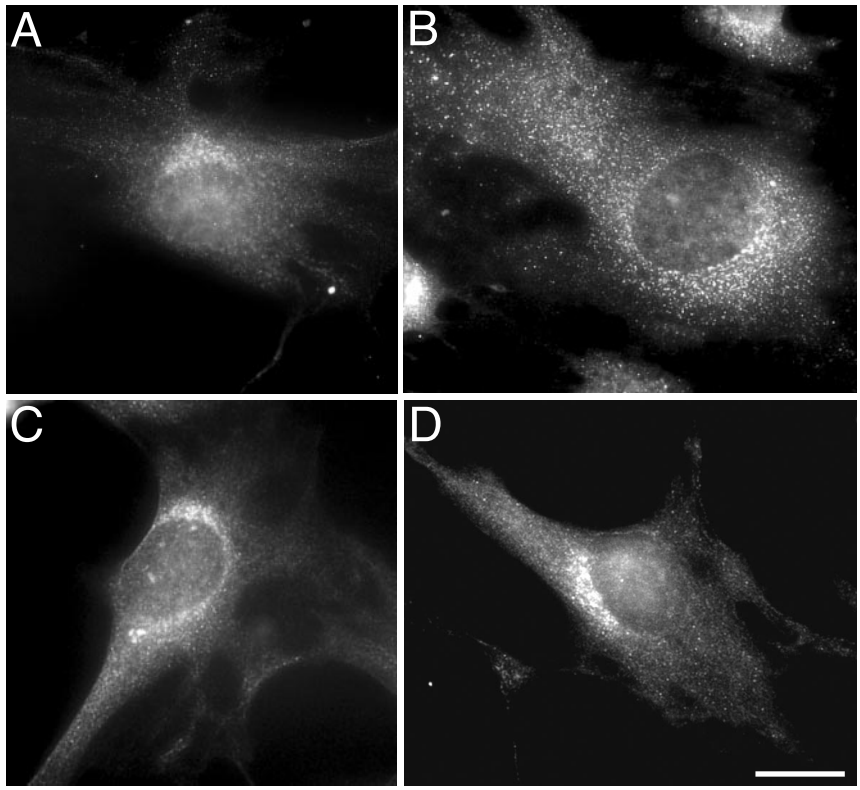

Figure 7. Tm5NM-2 localization is sensitive to nocodazole but not cytochalasin D treatment. Exposure of NIH3T3 cells to 30 μM nocodazole for 1 h resulted in dispersal of Tm5NM-2 throughout the cytoplasm into small puncta (B), whereas the vehicle had no effect (A). In contrast, treatment with 2 μM cytochalasin D for 1 h had no impact on the organization of Tm5NM-2 (D) compared with treatment with vehicle alone (C). Scale bars, 15 μm.

exposed perforated cells to jasplakinolide and quantitated vesicle numbers in the immediate vicinity of Golgi stacks (similar to those depicted in Figure 10, B and C), which were viewed by electron microscopy (unpublished data). In untreated preparations, there was an average of 80 vesicles in the immediate Golgi area, whereas jasplakinolide treatment increased this to 190 vesicles per stack (n = 15 Golgi stacks each condition). This suggests that actin polymer formation may be limiting for vesicle budding; the accumulation of vesicles upon actin polymerization might result from increased number of vesicles being formed (caught in the process of budding) or from increased retention of budded around the Golgi complex. Thus short actin filaments, defined by Tm5NM-2 and forming a Golgi-associated filament meshwork, has a role to play in vesicle budding.

DISCUSSION

In the present study we demonstrate a novel association of tropomyosin with a subset of Golgi-derived vesicles and therefore highlight a new role for tropomyosin in post-Golgi membrane trafficking in mammalian cells. Furthermore, we identify at least one of the Tm5NM isoforms (Tm5NM-2) previously reported to be associated with vesicles (Heimann *et al.*, 1999) and report that its restricted targeting to membranes is dictated by a sequence within an internal, alternatively spliced exon. We also show that both actin, in the form of short, Golgi-associated microfilaments, and Tm5NM-2 associate primarily with budding vesicles, suggesting a role for these microfilament proteins in vesicle generation.

Different antibodies raised against the 9d exon of the Tm5NM gene allowed the differentiation of Tm5NM-1 and -2 isoforms in cells. This revealed the striking restricted targeting of Tm5NM-2, labeled with the WS59/d antibody to the perinuclear Golgi complex, seen by immunofluorescence and immunogold labeling. In contrast Tm5NM-1 is targeted primarily to stress fibers. At the light microscopy level, Tm5NM-2 labeling was colocalized with both *cis*-Golgi markers (i.e., GM130) and TGN markers (p230). Ultrastructurally, Tm5NM-2 labeling was found associated with microfilaments and vesicles, which were clustered primarily around the TGN but could be seen at other points of vesicle budding across the Golgi stack.

There are numerous reports of distinct sorting patterns for different nonmuscle tropomyosin isoforms (Lin *et al.*, 1997; Gunning *et al.*, 1998a, 1998b). However the mechanism(s) underlying the differential targeting of tropomyosins are poorly understood. In the present study, we demonstrate that the different targeting of Tm5NM-2 and -1 in fibroblasts involves sequences within the internal alternatively spliced exons 6a and 6b. It is not clear, however, if the exons themselves contain the targeting sequences or whether the exons specifically interact with unknown targeted proteins. It may be, for example, that targeting to stress fibers in 3T3 cells is the default destination and targeting to the Golgi requires a Golgi-specific binding partner. Determination of these mechanisms in detail will provide an understanding of how the creation of functionally distinct actin filament populations has evolved.

What is the function of Tm5NM-2 on Golgi vesicles? That the membrane association of endogenous Tm5NM-2 is regulated by the ARF1 GTPase is suggested by its dissociation upon treatment with BFA. Exogenous EYFP-Tm5NM-2 localization was also BFA sensitive. The saturation or full occupancy of ARF-1–dependent binding sites may explain the slightly more diffuse staining of overexpressed EYFP-Tm5NM-2 (see Figures 3B and 6) compared with endogenous Tm5NM-2, which is tightly localized at the Golgi complex. The BFA results also suggest that the function of Tm5NM-2 at Golgi membranes is subject to regulation by

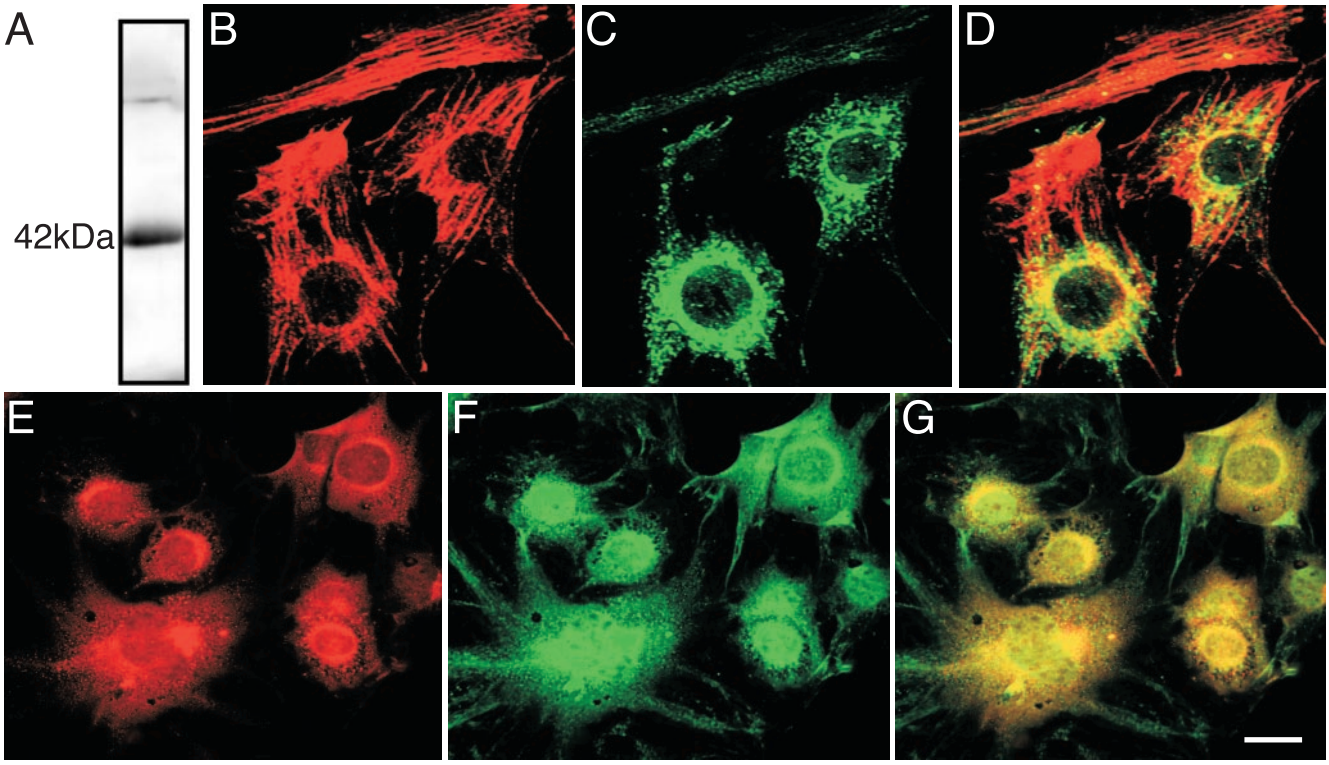

Figure 8. Anti-Gly245 antibody shows Golgi-like staining in NIH 3T3 fibroblasts. The anti-Gly245 actin antibody detects a single band at 42 kDa corresponding to both β- and γ-actin in a one-dimensional immunoblot. It sometimes detects a nonspecific slower migrating band (A). Confocal micrographs of the same optical section of NIH 3T3 fibroblasts double-labeled with anti–β-actin (B) and anti-gly245 (C) antibodies and merged image (D). β-actin characteristically detects stress fiber structures (B); however, anti-gly actin antibody preferentially detects puncta localized around the nucleus and in the cytoplasm and only weakly detects stress fibers (C and D). Anti-FTCD (E) and anti-gly245 (F) antibodies show overlapping subcellular distributions (G) in NIH 3T3 fibroblasts, suggesting that the anti-gly245 antibody may be labeling Golgi-associated actin. Scale bar, 10 μm.

ARF 1. Tm5NM-2 may be part of an actin-based tethering meshwork that is recruited by ARF1. The myosin motor, P200/myosinII, also associates with Golgi membranes in a BFA-sensitive manner (Narula *et al.,* 1992) and the work of Fucini *et al.,* 2000, 2002)shows that nonmuscle actin is bound to Golgi membranes by ARF1.

A well-known role in vitro and in vivo of tropomyosin is the stabilization of actin microfilaments against depolymer-

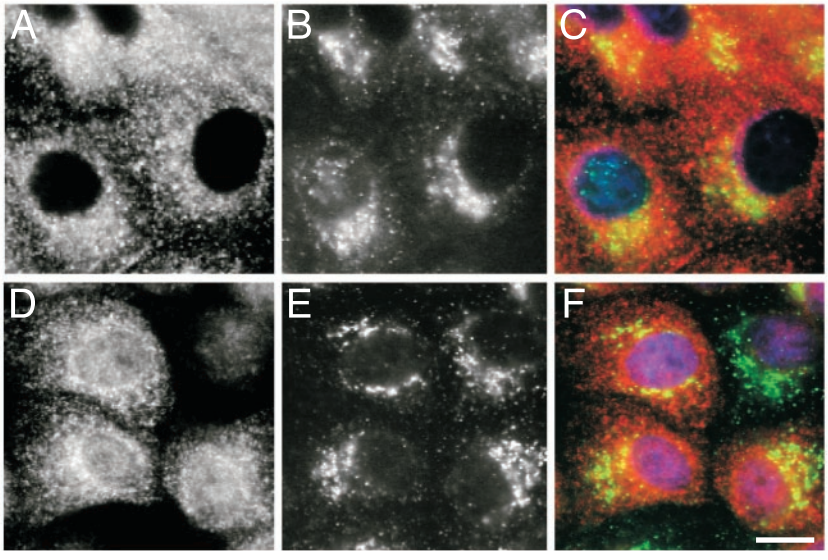

Figure 9. Short actin filaments and Tm5NM-2 localize to the Golgi complex in MDCK cells. Anti-Gly245 (A) and WS5/9d (D) were double-labeled with the TGN marker p230 on confluent MDCK cells. Both anti-Gly245 and WS5/9d localize to a perinuclear compartment overlapping with p230 (B and E). Merged images C and F show the regions of overlapping distributions. Scale bars, 15 μm.

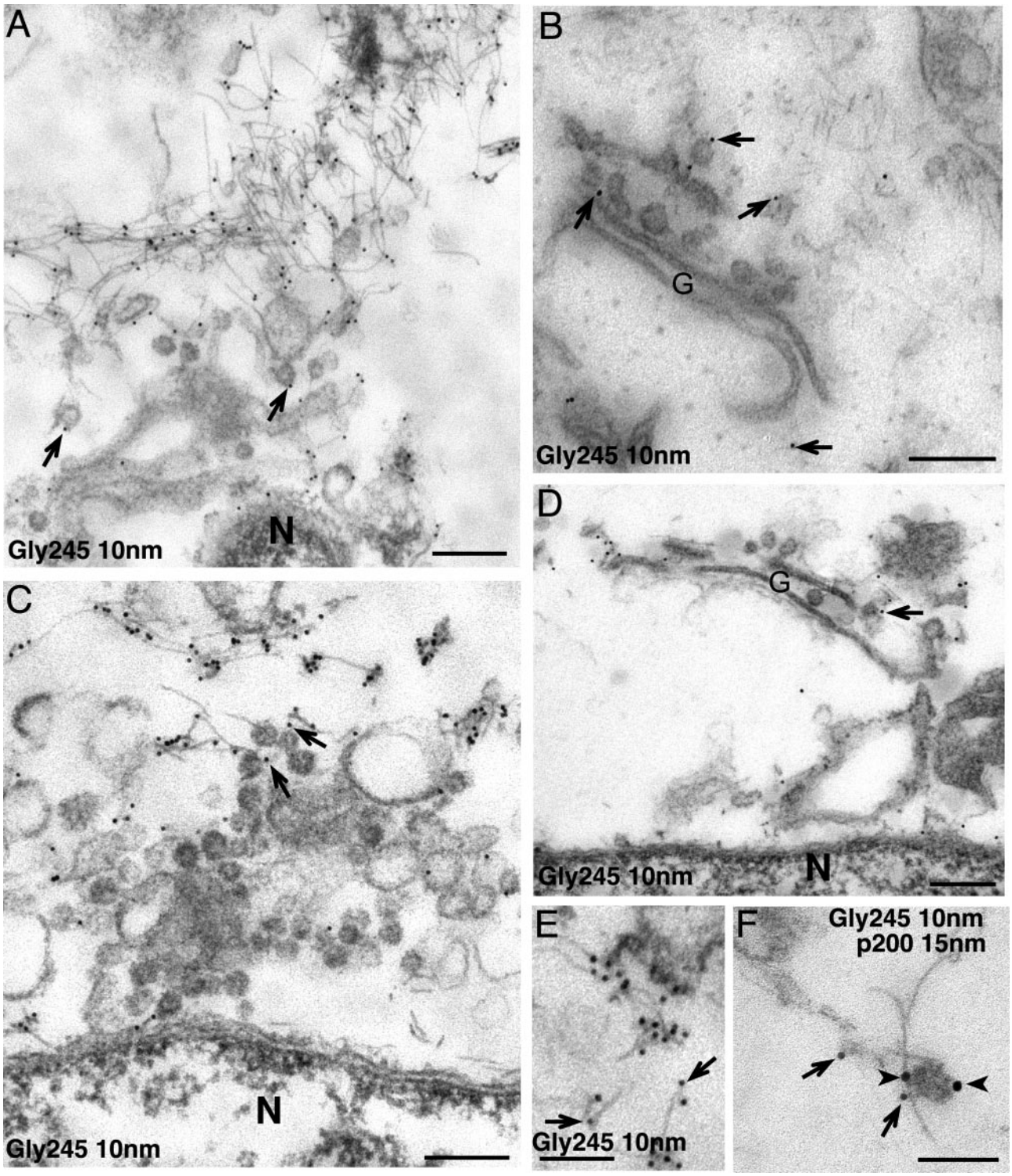

Figure 10. Immunogold labeling of Golgi-associated short microfilaments. Anti-gly245 labeling was performed on perforated MDCK cells where it specifically localizes on short microfilaments that were found clustered around Golgi stacks located in the perinuclear area (A and C). In some cases, anti-gly245 also labels vesicles seen budding from the Golgi complex (B and D). Anti-gly245 labeling is predominantly at the ends of microfilaments where these are easily depicted (E). Double-labeling shows conjoint association of anti-gly245 (arrows) and anti-p200/myosinII (arrowheads) labeling on a Golgi-derived vesicle attached to a short actin filament (F). N, nucleus; G, Golgi. Scale bars, 200 nm.

ization by its mode of binding to actin and by protecting against severing by ADF/cofilin (Broschat *et al.*, 1990; Bamburg 1999). Moreover, tropomyosin inhibits nucleation of new actin filaments by the Arp2/3 complex in vitro (Blanchoin *et al.*, 2001). The localization of Tm5NM-2 to vesicles may prevent further Arp2/3-mediated actin polymerization

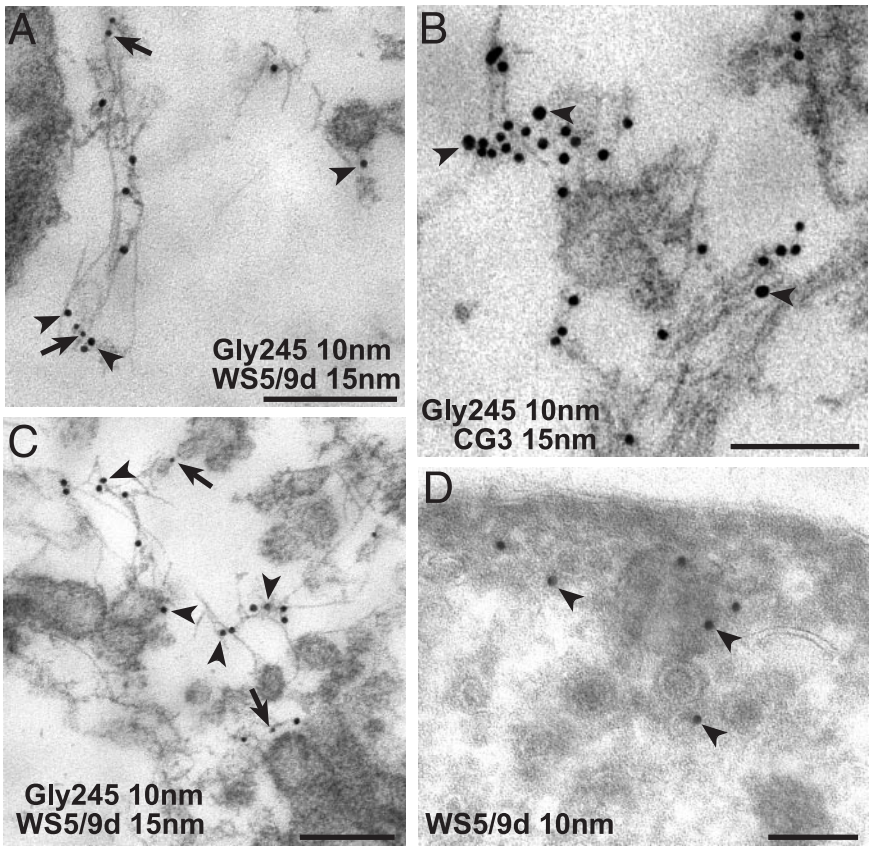

Figure 11. Tropomyosin isoforms localize on Golgi-associated microfilaments and vesicles. In perforated cells, Tm5NM isoforms (Tm5NM-2) labeled with either WS5/9d or CG3 antibodies (arrowheads) are associated with short actin filaments that are colabeled with anti-gly245 (arrows; A–C). These microfilaments are also often found attached to Golgi-derived vesicles (C). On cryosections of fixed cells, WS5/9d labeling is seen directly associated with the surface of coated vesicles in the cytoplasm (D). Scale bars, 200 nm.

on these vesicles leading to a stable vesicle cytoskeleton. Tm5NM-2 may protect vesicle associated filaments from depolymerization by ADF/cofilin and thus by controlling vesicle actin dynamics creates a stable carrier actin meshwork. Only those vesicles attached to tropomyosin-stabilized actin filaments may then be cross-linked (for example, by isoforms of β-spectrin other than βIII) to create tethered clusters of vesicles (De Matteis and Morrow, 1998). Alternatively, another property of tropomyosins is that they make actin filaments stronger by making them more rigid (Adami *et al.*, 2002). Tm5NM-2 stabilized actin filaments may be stronger and less flexible, thus providing sufficient mechanical strength for efficient vesicle generation/budding and/or later processes including tethering and short-range vesicle movement. Mutation or targeted inactivation of the *Drosophila melanogaster Tm II* gene inhibits targeting of oskar mRNA to the posterior pole of the oocyte (Erdelyi *et al.*, 1995; Tetzlaff *et al.*, 1996). These studies suggests that tropomyosin-stabilized filaments are required for local short-distance transport of mRNA. Tm5NM-2 may perform a similar role at the Golgi in facilitating short-range movements of carriers through stabilization of actin microfilaments.

Previous studies from this group and others have suggested roles for tropomyosin isoforms in intracellular trafficking pathways and organelle localization in yeast, fruit flies, and mammalian cells (Hegmann *et al.*, 1989; Liu and Bretscher, 1992; Erdelyi *et al.*, 1995; Pelham *et al.*, 1996; Pruyne *et al.*, 1998; Heimann *et al.*, 1999). Tm 3, but not Tm5NM-1, inhibited saltatory granule movement and caused lysosome mislocalization (Hegmann *et al.*, 1989; Pelham *et al.*, 1996). Evidence for a role of tropomyosin in post-Golgi trafficking has been reported in yeast. Tpm1p of *S. cerevisiae* is involved with Myo2p in the trafficking of post-Golgi carriers to sites of polarized growth along actin cables (Liu and Bretscher, 1992; Pruyne *et al.*, 1998). However, in contrast to Tm5NM-2 in mammalian cells, yeast Tpm1p is not found on vesicles and is required for the stability of actin cables, which form tracks along which Golgi vesicles translocate to sites of polarized growth. The *Tm5NM* gene is not found in yeast. Therefore *Tm5NM* and *TPM1* genes play quite different roles in post-Golgi trafficking in yeast and mammalian cells.

We also investigated actin distribution in this study. Two different antibodies to actin produced distinct staining patterns in cells. The anti-gly245 labeling was concentrated in the perinuclear region, particularly around the Golgi complex. Staining at the light microscopy level showed a lack of large microfilaments in this region, compared with the stress fibers stained with the β-actin antibody in the cell periphery. At an ultrastructural level, we confirmed that the anti-gly245 labeling was associated with the ends of short actin filaments, as predicted by the nature of its epitope. This staining thus reveals a novel population of Golgi-associated microfilaments that are distinct in structure and defined by specific binding proteins, such as Tm5NM-2. Furthermore we found that the anti-gly245 actin antibody preferentially detected membrane-associated actin filaments including actin on vesicles budding from Golgi membranes. This antibody is likely to prove a useful tool in studying membrane-bound actin because visualization by immunofluorescence of Golgi-associated actin has been notoriously difficult using standard reagents such as phalloidin. Taken together, the preferential association of both Tm5NM-2 and short actin filaments with budding structures and the ARF 1–regulated association of both Tm5NM-2 and actin (Godi *et al.*, 1998; Fucini *et al.*, 2000) suggests that these two microfilament

proteins are recruited to membranes in a regulated and dynamic manner to participate in vesicle budding. The high concentration of short actin filaments labeled with anti-gly245 and with Tm5NM antibodies in the vicinity of the Golgi complex suggests that this is a distinct population of microfilaments that is customized for a role in vesicle budding and trafficking.

Nonmuscle actin isoforms have been reported to be associated with Golgi-derived vesicles and cisternae (Heimann *et al.*, 1999; Valderrama *et al.*, 2000). Indeed multiple biochemically distinct pools of actin associate with Golgi membranes (Fucini *et al.*, 2000). Actin is involved in the positioning and morphology of the Golgi complex (Valderrama *et al.*, 1998). Actin has been implicated in detachment of post-Golgi carriers (Musch *et al.*, 1997; Stow *et al.*, 1998; Musch *et al.*, 2001). Exit from the Golgi complex of carriers containing VSV-G-GFP depended on an intact actin cytoskeleton (Hirschberg *et al.*, 1998). Latrunculin B delayed exit of apical (p75) and basolateral membrane-destined proteins (NCAM) from the TGN (Musch *et al.*, 2001). Disassembly of actin microfilaments, using latrunculin B or C2 toxin, slows BFA-induced redistribution of the Golgi into the ER (Valderrama *et al.*, 2001). Mutant Shiga toxin and the KDEL receptor are abnormally trafficked after microfilament depolymerization (Valderrama *et al.*, 2001). These studies using actin-disrupting toxins together with the long list of actin-binding proteins associated with Golgi membranes clearly implicate the actin microfilament system in Golgi to ER and post-Golgi transport. However, the exact role of actin remains elusive and is yet to be determined. Interestingly, we found the short, Golgi-associated actin filaments are not sensitive to depolymerization by cytochalsain D, perhaps helping to explain some of the varied effects of this drug in previous trafficking studies. Actin, based on studies of its binding partners, has been proposed to be involved in various mechanisms associated with vesicle budding at the level of the Golgi complex, including the generation of mechanical force for membrane extension or as part of a tethering meshwork to retain vesicles or finally for actual transport of carrier vesicles (Stow *et al.*, 1998; Lorra and Huttner, 1999; De Malteis and Morrow, 2000). The presence of actin and Tm5NM-2 on budding vesicles is consistent with the overall hypothesis that microfilaments are involved in budding. Our results point to specific roles in either facilitating membrane extension and vesiculation or in the tethering of fully formed carriers. Our work now provides a framework and useful molecular tools for future studies to address these issues.

ACKNOWLEDGMENTS

We thank colleagues where acknowledged for reagents, members of our laboratories for helpful discussions, and particularly Jeff Hook for help with final cell culture experiments. P.W.G. and J.L.S. are Principal Research Fellows of the National Health and Medical Research Council (NHMRC) of Australia. The work was supported by grants to P.W.G. and J.L.S. from the NHMRC and by support from the Australian Research Council, Special Research Centre for Functional and Applied Genomics at the IMB.

REFERENCES

Adami, R., Cintio, O., Trombelta, G., Choquet, D., and Grazi, E. (2002). Effects of chemical modification tropomyosin, and myosin subfragment 1 on the yield strength and critical concentration of F-actin. Biochemistry *41,* 5907–5912.

Bamburg, J.R. (1999). Proteins of the ADF/cofilin family: essential regulators of actin dynamics. Annu. Rev. Cell Dev. Biol. *15,* 185–230.

Beck, K.A., Buchanan, J.A., Malhotra, V., and Nelson, W.J. (1994). Golgi spectrin: identification of an erythroid beta-spectrin homologue associated with the Golgi complex. J. Cell Biol. *127,* 707–723.

Beck, K.A., Buchanan, J.A., and Nelson, W.J. (1997). Golgi membrane skeleton: identification, localization and oligomerization of a 195 kDa ankyrin associated with the Golgi complex. J. Cell Sci. *110,* 1239–1249.

Blanchoin, L., Pollard, T.D., and Hitchcock-DeGregori, S.E. (2001). Inhibition of the Arp2/3 complex-nucleated actin polymerization and branch formation by tropomyosin. Curr. Biol. *11,* 1300–1304.

Broschat, K.O. (1990). Tropomyosin prevents depolymerization of actin filaments from the pointed end. J. Biol. Chem. *265,* 21323–21329.

Brown, D.L., Heimann, K., Lock, J., Kjer-Nielsen, L., van Vliet, C., Stow, J.L., and Gleeson, P.A. (2001). The GRIP domain is a specific targeting sequence for a population of trans-Golgi network derived tubulo-vesicular carriers. Traffic *2,* 336–344.

Bryce, N.S.*et al.* (2003). Specification of actin filament function and molecular composition by tropomyosin isoforms. Mol. Biol. Cell *14,* 1002–1016.

Burgess, D.R., Broschat, K.O., and Hayden, J.M. (1987). Tropomyosin distinguishes between the two actin-binding sites of villin and affects actin-binding properties of other brush border proteins. J. Cell Biol. *104,* 29–40.

De Matteis, M.A., and Morrow, J.S. (2000). Spectrin tethers and mesh in the biosynthetic pathway. J. Cell Sci. *113,* 2331–2343.

Devarajan, P., Stabach, P.R., Mann, A.S., Ardito, T., Kashgarian, M., and Morrow, J.S. (1996). Identification of a small cytoplasmic ankyrin (AnkG119) in the kidney and muscle that binds beta I sigma spectrin and associates with the Golgi apparatus. J. Cell Biol. *133,* 819–830.

Dong, J., Radau, B., Otto, A., Mulle, E., Lindschau, C., and Westermann, P. (2000). Profilin I attached to the Golgi is required for the formation of constitutive transport vesicles at the trans-Golgi network. Biochim. Biophys. Acta *1497,* 253–260.

Drees, B., Brown, C., Barrell, B.G., and Bretscher, A. (1995). Tropomyosin is essential in yeast, yet the TPM1 and TPM2 products perform distinct functions. J. Cell Biol. *128,* 383–392.

Dufour, C., Weinberger, R.P., Schevzov, G., Jeffrey, P.L., and Gunning, P. (1998). Splicing of two internal and four carboxyl-terminal alternative exons in nonmuscle tropomyosin 5 pre-mRNA is independently regulated during development. J. Biol. Chem. *273,* 18547–18555.

Erdelyi, M., Michon, A.M., Guichet, A., Glotzer, J.B., and Ephrussi, A. (1995). Requirement for Drosophila cytoplasmic tropomyosin in oskar mRNA localization. Nature *377,* 524–527.

Fanning, A.S., Wolenski, J.S., Mooseker, M.S., and Izant, J.G. (1994). Differential regulation of skeletal muscle myosin-II and brush border myosin-I enzymology and mechanochemistry by bacterially produced tropomyosin isoforms. Cell Motil. Cytoskel. *29,* 29–45.

Fowler, V.M. (1996). Regulation of actin filament length in erythrocytes and striated muscle. Curr. Opin. Cell Biol. *8,* 86–96.

Fucini, R.V., Navarrete, A., Vadakkan, C., Lacomis, L., Erdjument-Bromage, H., Tempst, P., and Stamnes, M. (2000). Activated ADP-ribosylation factor assembles distinct pools of actin on golgi membranes. J. Biol. Chem. *275,* 18824–18829.

Fucini, R.V., Chen, J-L., Sharam, C., Kessels, M.M., and Stamnes, M. (2002). Golgi vesicle proteins are linked to the assembly of an actin complex defined by mAbp1. Mol. Biol. Cell *13,* 621–631.

Godi, A., Santone, I., Pertile, P., Devarajan, P., Stabach, P.R., Morrow, P.S., DiTullio, G., Polishchuk, R., Petrucci, T.C., Luini, A., and De Matteis, M.A. (1998). ADP ribosylation factor regulates spectrin binding to the Golgi complex. Proc. Natl. Acad. Sci. USA *95,* 8607–8612.

Gunning, P., Weinberger, R., Jeffrey, P., and Hardeman, E. (1998a). Isoform sorting and the creation of intracellular compartments. Annu. Rev. Cell Dev. Biol. 339–372.

Gunning, P., Hardeman, E., Jeffrey, P., and Weinberger, R. (1998b). Creating intracellular structural domains: spatial segregation of actin and tropomyosin isoforms in neurons. Bioessays *20,* 892–900.

Hannan, A.J., Schevzov, G., Gunning, P., Jeffrey, P.L., and Weinberger, R.P. (1995). Intracellular localization of tropomyosin mRNA and protein is associated with development of neuronal polarity. Mol. Cell. Neurosci. *6,* 397–412.

Hegmann, T.E., Lin, J.L., and Lin, J.J. (1989). Probing the role of nonmuscle tropomyosin isoforms in intracellular granule movement by microinjection of monoclonal antibodies. J. Cell Biol. *109,* 1141–1152.

Heimann, K., Percival, J.M., Weinberger, R., Gunning, P., and Stow, J.L. (1999). Specific isoforms of actin-binding proteins on distinct populations of Golgi-derived vesicles. J. Biol. Chem. *274,* 10743–10750.

Herman, I.M. (1993). Actin isoforms. Curr. Opin. Cell Biol. *5,* 48–55.

Hirschberg, K., Miller, C.M., Ellenberg, J., Presley, J.F., Siggia, E.D., Phair, R.D., and Lippincott-Schwartz, J. (1998). Kinetic analysis of secretory protein traffic and characterization of golgi to plasma membrane transport intermediates in living cells. J. Cell Biol. *143,* 1485–1503.

Ikonen, E., de Almeida, J.B., Fath, K.R., Burgess, D.R., Ashman, K., Simons, K., and Stow, J.L. (1997). Myosin II is associated with Golgi membranes: identification of p200 as nonmuscle myosin II on Golgi-derived vesicles. J. Cell Sci. *110,* 2155–2164.

Ishikawa, R., Yamashiro, S., and Matsumura, F. (1989). Differential modulation of actin-severing activity of gelsolin by multiple isoforms of cultured rat cell tropomyosin. Potentiation of protective ability of tropomyosins by 83-kDa nonmuscle caldesmon. J. Biol. Chem. *264,* 7490–7497.

Ishikawa, R., Hayashi, K., Shirao, T., Xue, Y., Takagi, T., Sasaki, Y., and Kohama, K. (1994). Drebrin, a development-associated brain protein from rat embryo, causes the dissociation of tropomyosin from actin filaments. J. Biol. Chem. *269,* 29928–29933.

Laemmli, U.K. (1970). Cleavage of structural proteins during the assembly of the head of bacteriophage T4. Nature *227,* 680–685.

Leavitt, J., Ng, S.Y., Aebi, U., Varma, M., Latter, G., Burbeck, S., Kedes, L., and Gunning, P. (1987). Expression of transfected mutant beta-actin genes: alterations of cell morphology and evidence for autoregulation in actin pools. Mol. Cell. Biol. *7,* 2457–2466.

Lees-Miller, J.P., and Helfman, D.M. (1991). The molecular basis for tropomyosin isoform diversity. Bioessays *13,* 429–437.

Lin, J.J., Warren, K.S., Wamboldt, D.D., Wang, T., and Lin, J.L. (1997). Tropomyosin isoforms in nonmuscle cells. Int. Rev. Cytol. *170,* 1–38.

Liu, H., and Bretscher, A. (1992). Characterization of TPMI disrupted yeast cells indicates an involvement of tropomyosins in directed vesicular transport. J. Cell Biol. *118,* 285–299.

Lorra, C., and Huttner, W.B. (1999). The mesh hypothesis of Golgi dynamics. Nat. Cell Biol. *1,* E113–E115.

Luna, A., Matas, O.B., Martinez-Menarguez, J.A., Mato, E., Duran, J.M., Ballesta, J., Way, M., and Egea, G. (2002). Regulation of protein transport from the Golgi complex to the endoplasmic reticulum by CDC42 and N-WASP. Mol. Biol. Cell *13,* 866–879.

Musch, A., Cohen, D., Kreitzer, G., and Rodriguez-Boulan, E. (2001) cdc42 regulates the exit of apical and basolateral proteins from the trans-Golgi network. EMBO J. *20,* 2171–2179.

Musch, A., Cohen, D., and Rodriguez-Boulan, E. (1997). Myosin II is involved in the production of constitutive transport vesicles from the TGN. J. Cell Biol. *138,* 291–306.

Miranda, K.C., Khromykh, T., Christy, P., Le, T.L., Gottardi, C.J., Yap, A.S., Stow, J.L., and Teasdale, R.D. (2001). A dileucine motif targets E-cadherin to the basolateral cell surface in Madin-Darby canine kidney and LLC-PK1 epithelial cells. J. Biol. Chem. *276,* 22565–22572.

Nakamura, N., Rabouille, C., Watson, R., Nilsson, T., Hui, N., Slusarewicz, P., Kreis, T, E., and Warren, G. (1995) Characterization of a cis-Golgi matrix protein, GM130. J. Cell Biol. *131,* 1715–1726.

Narula, N., McMorrow, I., Plopper, G., Doherty, J., Matlin, K.S., Burke, B., and Stow, J.L. (1992). Identification of a 200-kD, brefeldin-sensitive protein on Golgi membranes. J. Cell Biol. *117,* 27–38.

Ono, S., and Ono, K. (2002). Tropomyosin inhibits ADF/cofilin-dependent actin filament dynamics. J. Cell Biol. *156,* 1065–1076.

Pelham, R.J., Jr., Lin, J.J., and Wang, Y.L. (1996). A high molecular mass non-muscle tropomyosin isoform stimulates retrograde organelle transport. J. Cell Sci. *109,* 981–989.

Percival, J.M., Thomas, G., Cock, T.A., Gardiner, E.M., Jeffrey, P.L., Lin, J.J., Weinberger, R.P., and Gunning, P. (2000). Sorting of tropomyosin isoforms in synchronised NIH 3T3 fibroblasts: evidence for distinct microfilament populations. Cell Motil. Cytoskel. *47,* 189–208.

Phillips, G.N., Jr., Lattman, E.E., Cummins, P., Lee, K.Y., and Cohen, C. (1979). Crystal structure and molecular interactions of tropomyosin. Nature *278,* 413–417.

Pruyne, D.W., Schott, D.H., and Bretscher, A. (1998). Tropomyosin-containing actin cables direct the Myo2p-dependent polarized delivery of secretory vesicles in budding yeast. J. Cell Biol. *143,* 1931–1945.

Steinmetz, M.O., Stoffler, D., Hoenger, A., Bremer, A., and Aebi, U. (1997). Actin: from cell biology to atomic detail. J. Struct. Biol. *119,* 295–320.

Stow, J.L., Fath, K.R., and Burgess, D.R. (1998). Budding roles for myosin II on the Golgi. Trends Cell Biol. *8,* 138–141.

Strand, J., Nili, M., Homsher, E., and Tobacman, L.S. (2001). Modulation of myosin function by isoform-specific properties of Saccharomyces cerevisiae and muscle tropomyosins. J. Biol. Chem. *276,* 34832–34839.

Sung, L.A., Gao, K.M., Yee, L.J., Temm-Grove, C.J., Helfman, D.M., Lin, J.J., and Mehrpouryan, M. (2000). Tropomyosin isoform 5b is expressed in human erythrocytes: implications of tropomodulin-TM5 or tropomodulin-TM5b complexes in the protofilament and hexagonal organization of membrane skeletons. Blood *95,* 1473–1480.

Tang, N., and Ostap, E.M. (2001). Motor domain-dependent localization of myo1b (myr-1). Curr. Biol. *11,* 1131–1135.

Tetzlaff, M.T., Jackle, H., and Pankratz, M.J. (1996). Lack of Drosophila cytoskeletal tropomyosin affects head morphogenesis and the accumulation of oskar mRNA required for germ cell formation. EMBO J. *15,* 1247–1254.

Towbin, H., Staehelin, T., and Gordon, J. (1979). Electrophoretic transfer of proteins from polyacrylamide gels to nitrocellulose sheets: procedure and some applications. Proc. Natl. Acad. Sci. USA *76,* 4350–4354.

Valderrama, F., Babia, T., Ayala, I., Kok, J.W., Renau-Piqueras, J., and Egea, G. (1998). Actin microfilaments are essential for the cytological positioning and morphology of the Golgi complex. Eur. J. Cell Biol. *76,* 9–17.

Valderrama, F., Luna, A., Babia, T., Martinez-Menarguez, J.A., Ballesta, J., Barth, H., Chaponnier, C., Renau-Piqueras, J., and Egea, G. (2000). The golgi-associated COPI-coated buds and vesicles contain beta/gamma-actin. Proc. Natl. Acad. Sci. USA *97,* 1560–1565.

Valderrama, F., Duran, J.M., Babia, T., Barth, H., Renau-Piqueras, J., and Egea, G. (2001). Actin microfilaments facilitate the retrograde transport from the Golgi complex to the endoplasmic reticulum in mammalian cells. Traffic *2,* 717–726.

Vrhovski, B., Schevzov, G., Dingle, S., Lessard, J., Gunning, P., and Weinberger, R.P. (2003). Tropomyosin isoforms from the gamma gene differing at the C-terminus are spatially and developmentally regulated in the brain. J. Neurosci. Res. *72,* 373–383.

Weinberger, R., Schevzov, G., Jeffrey, P., Gordon, K., Hill, M., and Gunning, P. (1996). The molecular composition of neuronal microfilaments is spatially and temporarily regulated. J Neurosci. *16,* 238–252.

Wessel, D., and Flugge, U.I. (1984). A method for the quantative recovery of protein in dilute solution in the presence of detergents and lipids. Anal. Biochem. *138,* 141–143.

Wylie, F., Heimann, K., Le, T.L., Brown, D., Rabnott, G., and Stow, J.L. (1999). GAIP, a $G\alpha_{i\text{-}3}$-binding protein is associated with Golgi-derived vesicles and protein trafficking. Am. J. Physiol. *276,* C497–C506.